

Research Paper

Hypoxia-elicited mesenchymal stem cell-derived exosomes facilitates cardiac repair through miR-125b-mediated prevention of cell death in myocardial infarction

Ling-Ping Zhu^{1,6}, Tian Tian³, Jun-Yao Wang¹, Jing-Ni He¹, Tong Chen², Miao Pan¹, Li Xu¹, Hui-xin Zhang³, Xue-Ting Qiu², Chuan-Chang Li², Kang-Kai Wang⁴, Hong Shen⁵, Guo-Gang Zhang^{1,6}^{*}, Yong-Ping Bai^{2,6}^{*}

1. Department of Cardiovascular Medicine, Xiangya Hospital, Central South University, Changsha, China 410008
2. Department of Geriatric Medicine, Xiangya Hospital, Central South University, Changsha, China 410008
3. Department of Neurobiology, Nanjing Medical University, Nanjing, China 211166
4. Department of Pathophysiology, Xiangya School of Medicine, Central South University, Changsha, China 410008
5. Institute of Medical Sciences, Xiangya Hospital, Central South University, Changsha, China 410078
6. National Clinical Research Center for Geriatric Disorders, Xiangya Hospital, Central South University, Changsha, China, 410008

*These authors contributed equally to this article.

 Corresponding author: Dr. Yong-Ping Bai, Department of Geriatric Medicine, Xiangya Hospital, Central South University, Xiangya Road 87#, Changsha, China, 410008. Tel: 86-0731-84327695, Fax: 86-0731-84327695, E-mail: baiyongping@csu.edu.cn Or: Dr. Guo-Gang Zhang, Department of Cardiovascular Medicine, Xiangya Hospital, Central South University, Xiangya Road 87#, Changsha, China, 410008. Tel: 86-0731-84327695, Fax: 86-0731-84327695, E-mail: zhangguogang@csu.edu.cn

© Ivyspring International Publisher. This is an open access article distributed under the terms of the Creative Commons Attribution (CC BY-NC) license (<https://creativecommons.org/licenses/by-nc/4.0/>). See <http://ivyspring.com/terms> for full terms and conditions.

Received: 2018.06.20; Accepted: 2018.10.29; Published: 2018.11.29

Abstract

Exosomes (Exo) secreted from hypoxia-conditioned bone marrow mesenchymal stem cells (BM-MSCs) were found to be protective for ischemic disease. However, the role of exosomal miRNA in the protective effect of hypoxia-conditioned BM-MSCs-derived Exo (Hypo-Exo) remains largely uncharacterized and the poor specificity of tissue targeting of Exo limits their clinical applications. Therefore, the objective of this study was to examine the effect of miRNA in Hypo-Exo on the repair of ischemic myocardium and its underlying mechanisms. We further developed modified Hypo-Exo with high specificity to the myocardium and evaluate its therapeutic effects.

Methods: Murine BM-MSCs were subjected to hypoxia or normoxia culture and Exo were subsequently collected. Hypo-Exo or normoxia-conditioned BM-MSC-derived Exo (Nor-Exo) were administered to mice with permanent condition of myocardial infarction (MI). After 28 days, to evaluate the therapeutic effects of Hypo-Exo, infarction area and cardio output in Hypo-Exo and Nor-Exo treated MI mice were compared through Masson's trichrome staining and echocardiography respectively. We utilized the miRNA array to identify the significantly differentially expressed miRNAs between Nor-Exo and Hypo-Exo. One of the most enriched miRNA in Hypo-Exo was knockdown by applying anti-miR in Hypoxia-conditioned BM-MSCs. Then we performed intramyocardial injection of candidate miRNA-knockdown-Hypo-Exo in a murine MI model, changes in the candidate miRNA's targets expression of cardiomyocytes and the cardiac function were characterized. We conjugated Hypo-Exo with an ischemic myocardium-targeted (IMT) peptide by bio-orthogonal chemistry, and tested its targeting specificity and therapeutic efficiency via systemic administration in the MI mice.

Results: The miRNA array revealed significant enrichment of miR-125b-5p in Hypo-Exo compared with Nor-Exo. Administration of miR-125b knockdown Hypo-Exo significantly increased the infarction area and suppressed cardiomyocyte survival post-MI. Mechanistically, miR-125b knockdown Hypo-Exo lost the capability to suppress the expression of the proapoptotic genes *p53* and *BAK1* in cardiomyocytes. Intravenous administration of IMT-conjugated Hypo-Exo (IMT-Exo)

showed specific targeting to the ischemic lesions in the injured heart and exerted a marked cardioprotective function post-MI.

Conclusion: Our results illustrate a new mechanism by which Hypo-Exo-derived miR125b-5p facilitates ischemic cardiac repair by ameliorating cardiomyocyte apoptosis. Furthermore, our IMT-Exo may serve as a novel drug carrier that enhances the specificity of drug delivery for ischemic disease.

Key words: Hypo-Exo, Nor-Exo, miR-125b-5p, myocardial infarction, IMT-Exo, apoptosis

Introduction

Myocardial ischemia is the leading cause of mortality worldwide and is often responsible for sudden death [1]. A growing number of studies have demonstrated the therapeutic potential of bone marrow mesenchymal stem cells (BM-MSCs) [2]. MSCs are multipotent and, when transplanted into an ischemic heart, can differentiate into endothelial cells, vascular smooth muscle cells, and even cardiac-like myocytes [3]. Preclinical and clinical studies on MSCs have shown their promise for the repair and regeneration of cardiac tissues. However, the major hurdles of MSC-based therapies for ischemic heart disease (IHD) are the low survival of transplanted cells in the ischemic region and the risk of embolism. Endogenous factors, such as the recipient's inflammatory response, may also contribute to the challenge of MSC-based therapies [4]. Interestingly, an increasing number of studies found that MSC-secreted exosomes (Exo) exhibit functions similar to those of MSCs [5,6]. Therefore, MSC-derived Exo may be harnessed as a new and alternative approach for the treatment of IHD.

Exo are 40-150 nm extracellular vesicles of endosomal origin and are secreted by all cell types [7,8]. Exo are surrounded by a bilayer lipid membrane that can protect their contents from degradation and allow the transfer of signaling molecules between cells and tissues [9]. As such, numerous studies have explored the role of Exo in ischemic diseases as a mediator for different cell types [10,11,12,13]. A recent study suggests that a direct transfer of stable and functional CD34⁺ exosomal miR-126-3p enhances angiogenesis in a mouse model of hindlimb ischemia [14].

Notably, MSC-derived Exo exhibit distinct functions due to differences in MSCs microenvironments [15]. One recent study indicates that Exo isolated from MSCs grown in medium similar to the environment of peripheral arterial disease (0% FBS, 1% O₂) contain a panel of pro-angiogenic factors that may be salutary for tissue ischemia. Indeed, hypoxia-conditioned BM-MSCs-derived Exo (Hypo-Exo) possess components that facilitate ischemic tissue recovery

[16]. Although most of the current studies on Exo have profiled the protein and RNA content [16], the miRNA content in Hypo-Exo and the underlying mechanisms by which these miRNAs contribute to ischemic heart repair *in vivo* remain unclear.

Exo manifest several favorable features, such as low immunogenicity, reduced biodegradability, low toxicity, natural encapsulation of endogenous bioactive molecules, and optimal protection of cargo [17,18]. However, recent biodistribution studies of unmodified Exo after intravenous injection show rapid accumulation in mononuclear phagocyte system (MPS) organs, such as the liver and spleen, and very few reach the heart after systemic administration [19,20]. Thus, the targeting characteristics of Exo require improvements before they can be used for therapeutic delivery for myocardial infarction.

The targeting specificity of Exo can be enhanced by surface modifications. Recently, several reports demonstrated that Exo can be modified using biochemical conjugation, a process known as the "Exo engineering" method [21,22,23]. Tian *et al.* found that the c(RGDyK) peptide can be easily and rapidly conjugated to the Exo surface via bio-orthogonal chemistry. Furthermore, they found that c(RGD)-Exo were enriched in the ischemic lesions of an affected brain following systemic administration [24].

Nowadays, myocardial reperfusion using either percutaneous coronary intervention or thrombolytic therapy is the standard treatment for acute myocardial infarction (MI). However, there are still 15–25% patients who are not reperfused in a timely manner due to contraindications or logistic issues [25]. In order to mimic this clinical situation, in the present study, we investigated the beneficial role of Hypo-Exo in cardiac repair using a mouse permanent MI model. We also performed a miRNA array and found that Hypo-Exo is enriched with miR-125b-5p, which exhibits an anti-apoptotic effect *in vivo* and *in vitro*. We showed that knockdown (KD) of miR-125b-5p in Hypo-Exo, by promoting apoptosis of cardiomyocytes, augments the size of the ischemic lesions in mice subjected to left ascending artery

ligation. Furthermore, we improved the targeted delivery of Hypo-Exo by conjugating them with a "CSTSMKAC" peptide (a derivative of the ischemic myocardium-targeted (IMT) peptide) as employed by several studies [26], and tested the therapeutic efficiency of these Exo via systemic administration in the mouse MI model.

Methods

An expanded methods section is available in Supplementary Material.

Exo isolation and characterization

α -minimal essential medium (α -MEM) containing 20% FBS was centrifuged at 200,000 $\times g$ for 18 h to deplete Exo. MSCs from passages 4-6 were cultured using 10% Exo-removed FBS for Exo collection. 2×10^6 MSCs were cultured in 100 mm dishes in normoxia and hypoxia condition for 72 h and 10 mL supernatant was collected. Exo were then isolated from the harvested supernatant according to a previous study [27]. Briefly, the supernatant was centrifuged at 300 $\times g$ for 10 min, 1200 $\times g$ for 20 min, then 10,000 $\times g$ for 30 min at 4 °C and then filtered using a 0.22 μm filter (Millipore, Billerica, MA, USA) to remove cells and debris. The filtrate was centrifuged at 140,000 $\times g$ for 90 min at 4 °C using a Type Ti70 rotor using an L-80XP ultracentrifuge (Beckman Coulter, Brea, CA, USA). Applying PBS to resuspend the Exo pellet and centrifuged again at 140,000 $\times g$ for 90 min. Afterwards, the pelleted Exo were resuspended in PBS and tested using a BCA Protein Assay kit (Thermo Fisher Scientific, USA). To detect Exo markers and the negative markers, Western blotting was applied with anti-Alix and anti-TSG101 antibodies (Abcam, Cambridge, UK) [28].

Mouse myocardial infarction (MI) model

Animal care and experimental procedures were approved by the Animal Research Committee of Central South University. Mice (C57BL/6, 6-8 weeks, 18-25 g) were anesthetized by intraperitoneal injection of pentobarbital sodium (60 mg/kg), ventilated via tracheal intubations connected to a rodent ventilator, and subjected to MI by ligation of the left anterior descending coronary artery using an 8-0 nylon suture. Echocardiographic studies were performed 28 days after MI using a Vevo 2100 ultrasound system (VisualSonics) [29].

Co-culture of Exo and cells

To investigate the role of exosomal miR-125b on H9C2 cells, 50 $\mu g/mL$ of the Exo isolated from miR125b knockdown hypoxia-conditioned BM-MSCs (miR-125b^{KD}-Hypo-Exo) or the Exo from negative

control-hypoxia-conditioned BM-MSCs (NC-Hypo-Exo) were incubated with H9C2 cells at 37 °C for 24 hrs. Then, the cells were subjected to hypoxia for 2 h and apoptosis was measured by flow cytometry, proliferation by cell counting kit-8 (CCK8) and target expression by Western blotting or qRT-PCR. To test the uptake of IMT-conjugated Hypo-Exo (IMT-Exo) by H9C2 cells, Hypoxia H9C2 cells were incubated with 50 $\mu g/mL$ of Cy5.5 labeled scrambled control modified Hypo-Exo (Cy5.5-Scr-Exo) or Cy-5.5 labeled IMT-Exo (Cy5.5-IMT-Exo) at 37 °C for 0.5 h. During the last 5 min, DAPI (5 $\mu g/mL$) was applied to stain cell nuclei. Fluorescence images were captured by confocal microscopy and processed and analyzed using ImageJ software.

Conjugation of ligands to Exo

Reactive dibenzylcyclooctyne (DBCO) were merged in amine-containing molecules on Exo applying a hetero-bifunctional crosslinker. 3 μM dibenzocyclooctyne-sulfo-N-hydroxysuccinimidyl ester (DBCO-sulfo-NHS; Sigma, St. Louis, MO, USA) was added to 0.5 mg/mL Exo in PBS and react at RT for 4 hrs. The DBCO-conjugated Exo (DBCO-Exo) were then ready for interact with azide-containing molecules via copper-free click chemistry. IMT peptide (CSTSMKAC) and scrambled IMT peptide (CSKTALSMC) with an azide group on the lysine were purchased from SciLight Biotechnology Co. (Beijing, China). Cy5.5 azide was purchased from Sigma (USA). Specifically, 0.3 μM IMT peptide or scrambled IMT peptide with azide was added to DBCO-Exo in PBS, and subsequently added 0.3 μM Cy5.5 azide if needed. The reaction was performed on a rotating mixer at 4 °C for 12 h. Then, floated the Exo on a 30% sucrose/D2O cushion and centrifuged at 164,000 $\times g$ for 90 min using a SW41Ti rotor (Beckman Coulter) to remove uncombined ligands. After washing with PBS, the IMT-Exo were resuspended and stored at -80 °C for further use. To assess the successful conjugation of Exo and IMT peptide, Cy5.5-conjugated Exo were applied to coverslips and imaged by fluorescence microscopy (Leica, USA). 0.5% BSA as an unmodified control was imaged [24].

Statistical analyses

The data are presented as mean \pm SEM. In comparisons of two groups, 2-tailed Student's t-test was used for parametric data, and Mann-Whitney U-test for non-parametric data. LSD method was used for multiple comparisons when a statistically significant difference was found. All experiments were repeated at least 3 times, and representative experiments are shown. Differences were considered significant at $P < 0.05$.

Results

Preparation and characterization of Hypo-Exo

Mouse BM-MSCs were isolated and cultured for 72 h under one of the following two culture conditions: normoxic (10% FBS, 21% O₂) and hypoxic preconditioning (10% FBS, 1% O₂). Exo were isolated from their conditioned medium by ultracentrifugation. We examined the diameter of both types of the MSC-derived Exo using transmission electron microscopy. Normoxia-conditioned BM-MSC-derived Exo (Nor-Exo) and Hypo-Exo were identified to have diameters of 40-150 nm (Figure 1A). Next, the morphology of Nor-Exo and Hypo-Exo was assessed by laser scattering microscopy (LSM) (Figure 1B-C). Nor-Exo was round in shape, with an average diameter of 107.3 ± 6.45 nm, while the mean diameter of Hypo-Exo was slightly larger at 136.5 ± 4.05 nm. Western blot analysis showed that the levels of TSG101 and Alix (known exosomal markers) were enriched in Hypo-Exo but were less pronounced in Nor-Exo, and almost no expression was observed in the supernatant of both the normoxic and hypoxic conditioned medium (Figure 1D).

Intramyocardial delivery of Hypo-Exo reduces the infarct size and improves cardiac function

To test the therapeutic effect of Hypo-Exo, we made an acute MI mouse model via permanent left anterior descending artery ligation as previously described [29]. Hypo-Exo was intramyocardially

administered to mice at the time of MI, whereas sham, PBS and Nor-Exo served as controls (Figure 2A). Histological analyses of the hearts 4 weeks post-MI indicated that mice injected with Hypo-Exo had a smaller infarct size than PBS-injected mice (6.60% ± 0.98% vs. 42.37% ± 6.96%, *P*<0.01) or Nor-Exo-injected mice (6.60% ± 0.98% vs. 15.83% ± 1.475%, *P*<0.01) (Figure 2B). To evaluate whether Hypo-Exo enhances cardiac repair post-MI, we measured myocardial contractile parameters at 28 d after MI. Echocardiography (Figure 2C-D) revealed that Hypo-Exo treatment reduced left ventricular injury, as indicated by the end systolic chamber volume (ESCV) and end systolic left ventricular internal diameter (LVID), compared with the PBS or Nor-Exo treatments (ESCV: 62.73 ± 1.46 μL vs. 85.00 ± 2.89 μL and 74.33 ± 2.33 μL, *P*<0.01 and *P*<0.05, respectively; LVID: 2.97 ± 0.09 mm vs. 4.77 ± 0.15 mm and 3.60 ± 0.06 mm, both *P*<0.01). By contrast, Hypo-Exo improved systolic function compared with the PBS and Nor-Exo controls, as indicated by the higher ejection fraction (EF%) and fraction shortening (FS%) (EF%: 49.67% ± 0.88% vs. 26.33% ± 2.03% and 40.67% ± 1.76%, *P*<0.01 and *P*<0.05, respectively; FS%: 31.67% ± 0.88% vs. 15.33% ± 1.76% and 23.67% ± 2.03%, *P*<0.01 and *P*<0.05, respectively).

Hypo-Exo is enriched with the antiapoptotic miR-125b-5p

To identify factors and the mechanism responsible for the beneficial effects of Hypo-Exo, we examined the exosomal miRNA content. We isolated

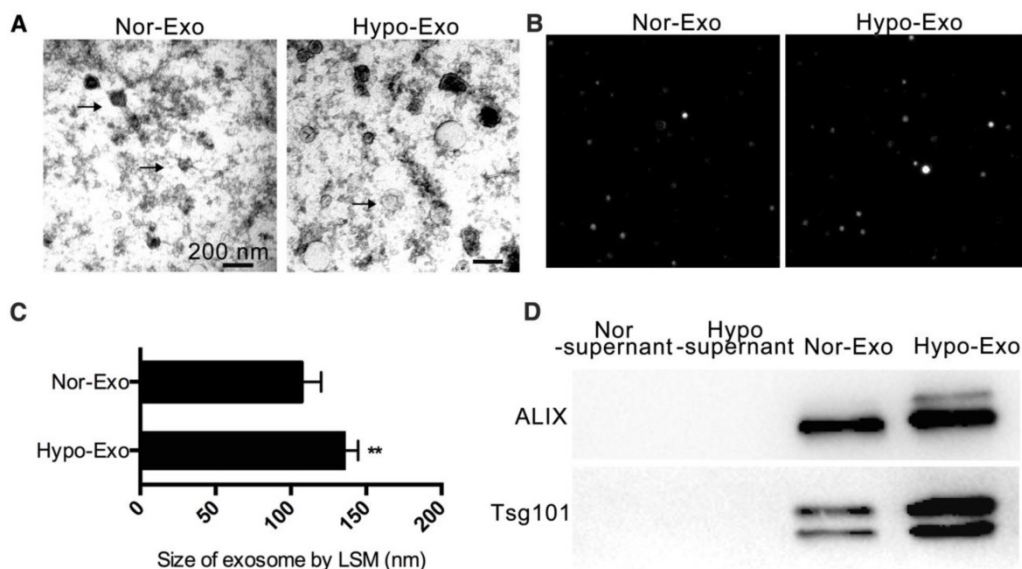


Figure 1. Characterization of Nor-Exo and Hypo-Exo. (A) Transmission electron micrographs of Nor-Exo and Hypo-Exo. Scale bar, 200 nm. Arrows, representative Exo. (B) Representative light scattering microscopy (LSM) images of Nor-Exo and Hypo-Exo. (C) Size distribution of Nor-Exo and Hypo-Exo based on LSM images. (D) Western blot analysis of Alix and TSG101 expression in Nor-Exo and Hypo-Exo. Supernatants obtained during Exo isolation by ultracentrifugation were used as negative controls. ***P*<0.01 for Hypo-Exo vs. Nor-Exo. Nor-Exo: normoxia-conditioned bone marrow mesenchymal stem cells-derived exosome; Hypo-Exo: hypoxia-conditioned bone marrow mesenchymal stem cells-derived exosome.

RNA from Hypo-Exo and Nor-Exo, performed microarray profiling of the miRNAs in the Exo, and compared the content between the two groups. Because Exo carry cell-specific proteins or mRNAs/miRNAs that mediate their biological effect, we focused on the miRNAs upregulated in Hypo-Exo compared with Nor-Exo. The miRNA microarray analysis (Figure 3A) showed the significantly upregulated miRNAs in Hypo-Exo (>3-fold, $q < 0.5$).

Based on the miRNA profiling data from microarray sequencing, we further validated the expression of the 12 upregulated miRNAs by qRT-PCR according to their low q -values. In all, 6 miRNAs—*mmu-miR-5112* ($P < 0.05$), *mmu-miR-711* ($P < 0.05$), *mmu-miR-125b* ($P < 0.01$), *mmu-miR-92a* ($P < 0.05$), *mmu-miR-7025* ($P < 0.01$) and *miR-7045* ($P < 0.05$)—of the 12 were significantly upregulated in Hypo-Exo compared with Nor-Exo (Figure 3B).

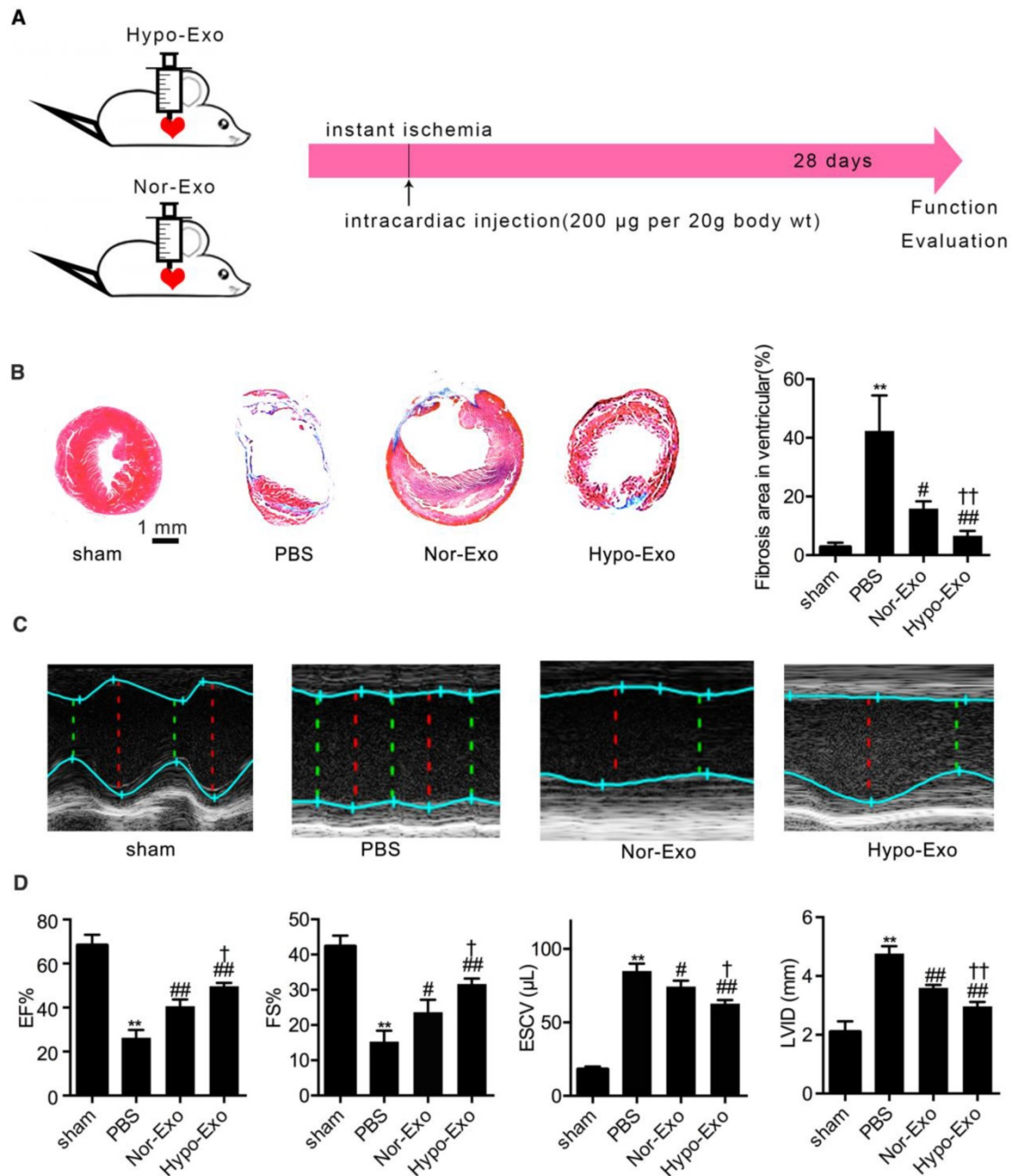


Figure 2. Enhanced cardiac function after myocardial infarction in mice transplanted with Hypo-Exo. (A) Schematic of the intracardiac injection with Nor-Exo and Hypo-Exo in a mouse model of MI. **(B)** Masson's trichrome-stained myocardial sections at 28 days from MI mice treated with sham, PBS, Nor-Exo, or Hypo-Exo. Scar tissue and viable myocardium are identified in blue and red, respectively. Scale bar, 1 mm. The bar chart on the right quantifies the extent of fibrosis in each treatment group. **(C-D)** Representative M-mode images (C) and quantification (D) of EF%, FS%, ESCV, and LVID measured by echocardiography of sham, PBS-treated, Nor-Exo-treated, and Hypo-Exo-treated mice at 28 days after MI. * $P < 0.05$, ** $P < 0.01$ for PBS vs. sham; # $P < 0.05$, ## $P < 0.01$ for Nor-Exo or Hypo-Exo vs. PBS; † $P < 0.05$, †† $P < 0.01$ for Hypo-Exo vs. Nor-Exo. MI: myocardial infarction. EF%: ejection fraction%; FS%: fraction shortening%; ESCV: end systolic chamber volume; LVID: left ventricular internal diameter.

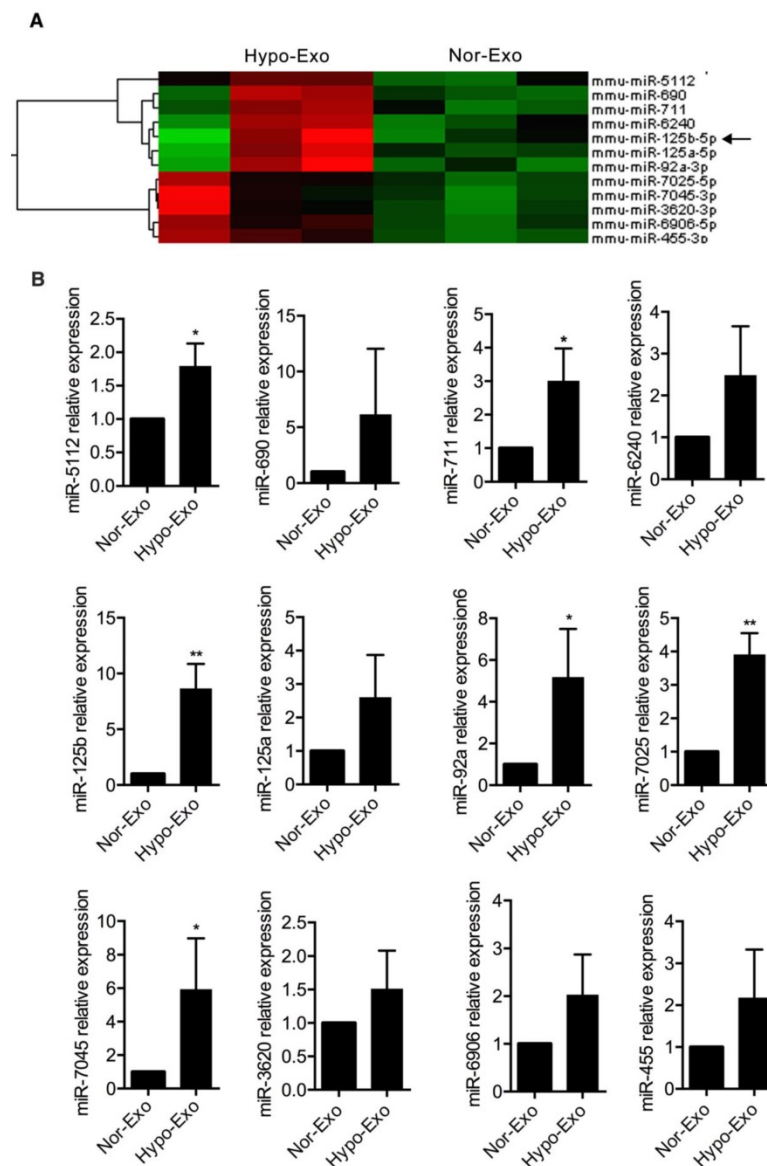


Figure 3. Profiling and identification of upregulated miRNAs in Nor-Exo and Hypo-Exo. (A) Heat map and supervised hierarchical clustering of the 12 upregulated miRNAs with a ≥ 3 -fold difference between Hypo-Exo and Nor-Exo. **(B)** Comparison of mmu-miR-5112, 690, 711, 125b, 3620, 6240, 125a, 6906, 92a, 7025, 7045, and 455 between Nor-Exo and Hypo-Exo from 3 independent experiments by RT-PCR. * $P < 0.05$. ** $P < 0.01$ for Hypo-Exo vs. Nor-Exo.

Decreased miR-125b-5p expression impairs Hypo-Exo-mediated cardioprotection

To gain further mechanistic insights into the role of exosomal miR-125b-5p in Hypo-Exo-induced cardioprotection in the murine MI model, miR-125b-5p loss-of-function studies were performed in Hypo-MSCs. We knocked down miR-125b expression using miR-125b anti-miR, and administered negative anti-miR controls. Exo were then isolated from the resulting conditioned medium. As shown in **Figure 4A**, the Exo isolated from miR125b KD hypoxia conditioned MSCs (miR125b^{KD}-Hypo-Exo) had decreased expression of miR-125b-5p compared with the Exo isolated from negative control-hypoxia conditioned MSCs

(NC-Hypo-Exo) (0.1670 ± 0.01 -fold, $P < 0.01$). miR125b^{KD}-Hypo-Exo or NC-Hypo-Exo was injected at multiple points into the infarct area at the time of MI induction. At 28 days post MI, transduction of the MI areas with miR125b^{KD}-Hypo-Exo resulted in decreased miR-125b-5p expression compared with that in mice injected with NC-Hypo-Exo (0.7333 ± 0.107 , $P < 0.05$, **Figure 4B**). As shown in **Figure 4C**, mice treated with miR125b^{KD}-Hypo-Exo showed a larger increase in the scarred area ($20.82\% \pm 1.34\%$ vs. $13.43\% \pm 1.81\%$, $P < 0.05$). Furthermore, **Figure 4D** shows that miR125b^{KD}-Hypo-Exo-treated mice had a significantly decreased EF% ($43.00\% \pm 2.08\%$ vs. $52.33\% \pm 1.86\%$, $P < 0.05$) and FS% ($22.33\% \pm 2.96\%$ vs. $32.67\% \pm 2.19\%$, $P < 0.05$), with a higher ESCV (77.67 ± 1.45 μL vs. 70.00 ± 1.16 μL , $P < 0.05$) and LVVID (3.300

± 0.17 mm vs. 2.667 ± 0.09 mm, $P < 0.05$) compared with NC-Hypo-Exo-treated mice. As cardiomyocyte apoptosis contributes to MI injury, and miR-125b is a known anti-apoptotic miRNA [30,31], we tested the effect of miR125b^{KD}-Hypo-Exo on MI-induced

myocardial apoptosis. **Figure 4E** illustrates that in miR125b^{KD}-Hypo-Exo-treated mice, apoptotic cells were significantly increased in the border zone (BZ) compared to apoptosis in the NC-Hypo-Exo-treated mice (24.67 ± 2.60 vs. 12.33 ± 2.85 , $P < 0.05$).

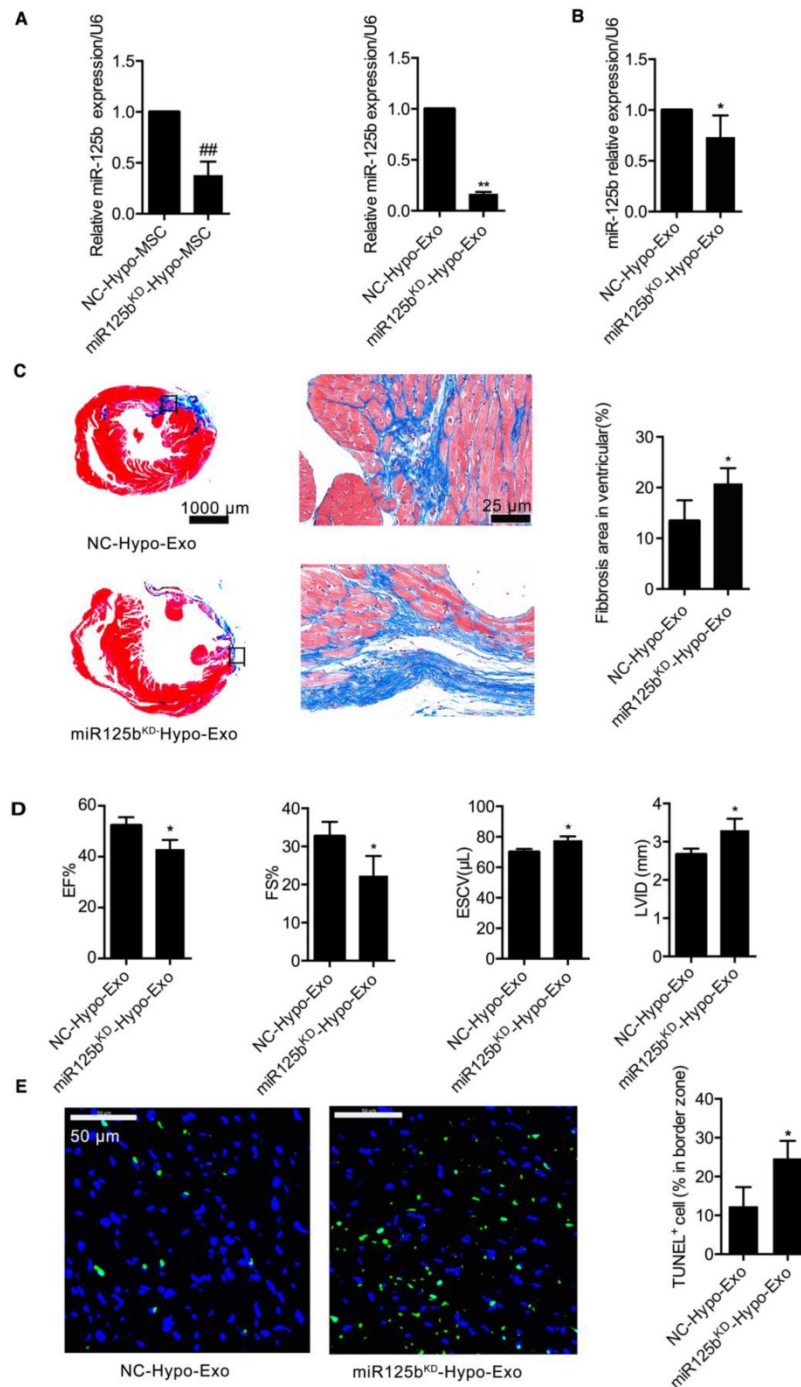


Figure 4. Inhibition of miR-125b in Hypo-Exo increase infarct size in a mouse model of MI. (A) miR-125b-5p expression was detected by RT-PCR in MSCs or in Exo isolated from the hypoxic medium of MSCs treated with 100 nmol inhibitor-125b or negative control (NC). **(B)** Expression of miR-125b in ischemic heart tissue after local injection of miR125b^{KD}-Hypo-Exo or NC-Hypo-Exo into the heart after left anterior descending artery ligation. **(C)** Representative Masson's trichome-stained images and statistical analysis of infarct area from mice administered miR125b^{KD}-Hypo-Exo or NC-Hypo-Exo. Assessment was performed at 28 days post-MI. Scale bar, 1 mm. **(D)** Quantification of EF%, FS%, ESCV, and LVID measured by echocardiography of miR125b^{KD}-Hypo-Exo-treated and NC-Hypo-Exo-treated mice at 28 days post-MI. **(E)** Representative immunofluorescence staining and quantification of TUNEL (green) in the ischemic regions of hearts treated with miR125b^{KD}-Hypo-Exo or NC-Hypo-Exo. Assessment was performed 28 days after ligation. Blue, DAPI. Scale bar, 50 μ m. n=6 mice per group. ###P < 0.01 for miR125b^{KD}-Hypo-Exo vs. NC-Hypo-Exo; *P < 0.05, **P < 0.01 for miR125b^{KD}-Hypo-Exo vs. NC-Hypo-Exo. KD: knockdown; miR125b^{KD}-Hypo-Exo: Exo from miR125b KD hypoxia-conditioned MSCs; NC-Hypo-Exo: Exo from negative control-hypoxia-conditioned MSCs.

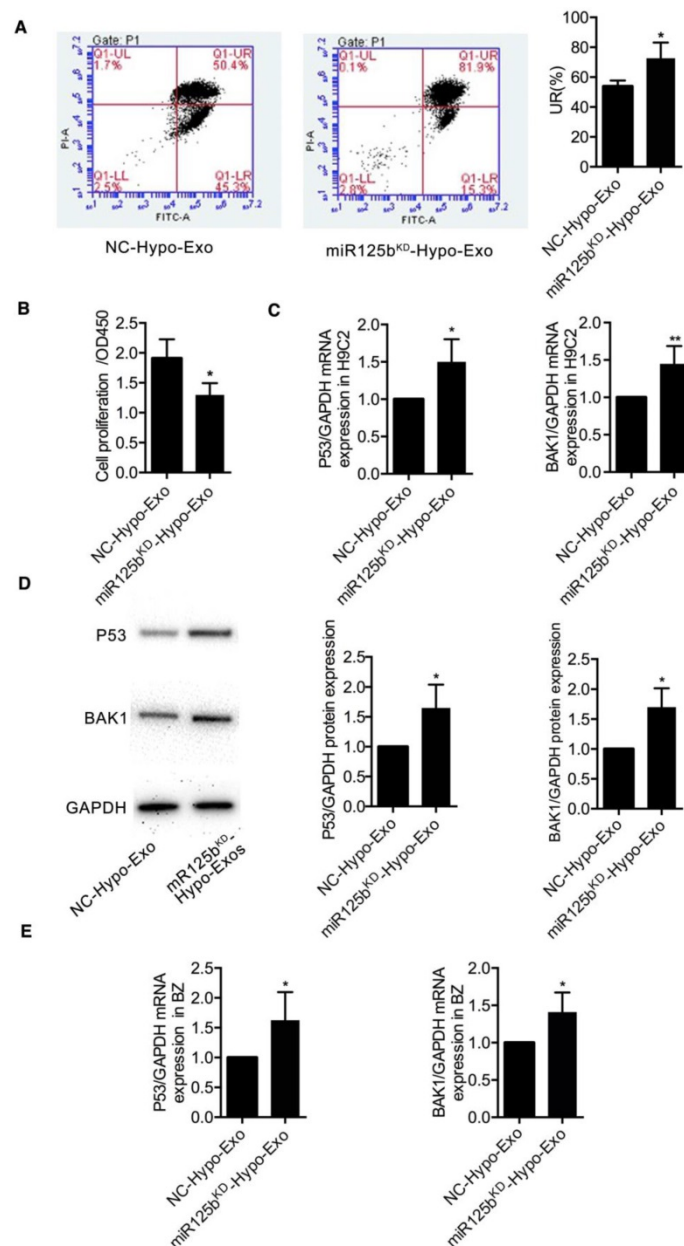


Figure 5. The effects of miR125b^{KD}-Hypo-Exo on the apoptosis and proliferation of H9C2 cells and changes in its targets' expression levels. (A-B) The effects of miR125b^{KD}-Hypo-Exo on H9C2 cell apoptosis (A) and proliferation (B) as determined by flow cytometry and CCK8 assay, respectively. **(C-D)** The effects of exosomal miR-125b on p53 and BAK1 mRNA (C) and protein (D) expression in H9C2 cells treated with miR125b^{KD}-Hypo-Exo or NC-Hypo-Exo. **(E)** The effects of exosomal miR-125b on p53 and BAK1 mRNA expression in the ischemic regions of hearts treated with miR125b^{KD}-Hypo-Exo or NC-Hypo-Exo. Each experiment was repeated 3 times. *P<0.05, **P<0.01 for miR125b^{KD}-Hypo-Exo vs. NC-Hypo-Exo.

miR-125b-5p is critical for Hypo-Exo-mediated protection of injured H9C2 cardiomyoblasts

To determine whether miR-125b contributes to the protective effects of Hypo-Exo against hypoxia-induced cell injury, miR-125b^{KD}-Hypo-Exo studies were performed in hypoxia injured H9C2 cells. miR-125b^{KD}-Hypo-Exo or their NC-Hypo-Exo were administered to cells before the cultures were subjected to hypoxia. As shown in Figure 5A and 5B, compared with the NC-Hypo-Exo, miR125b^{KD}-Hypo-Exo significantly increased the

percentage of late apoptotic cells (UR%), as revealed by flow cytometry analysis (Figure 5A; 72.67 ± 6.042 vs. 53.77 ± 2.275 , $P < 0.05$) and decreased proliferation, as determined by the CCK8 assay (1.298 ± 0.114 vs. 1.908 ± 0.184 ; $P < 0.05$).

To understand the mechanism by which miR-125b^{KD}-Hypo-Exo impaired Hypo-Exo-mediated H9C2 survival in the hypoxic environment, we examined the protein and mRNA levels of proapoptotic effectors, including the direct targets of miR-125b-5p: p53 and BAK1 [32,33]. As shown in **Figure 5C-D**, we observed a significant increase in the

mRNA and protein levels of *p53* (both $P < 0.05$) and *BAK1* ($P < 0.01$ and $P < 0.05$, respectively) in miR125b^{KD}-Hypo-Exo compared with control cells. Furthermore, to determine the mechanism by which miR125b^{KD}-Hypo-Exo attenuated myocardial apoptosis *in vivo*, we examined the mRNA levels of proapoptotic targets *p53* and *BAK1* in the myocardium of BZ. Compared with the NC-Hypo-Exo-treated myocardium, the miR125b^{KD}-Hypo-Exo-treated myocardium exhibited significantly increased mRNA expression of *p53* and *BAK1* (Figure 5E, $P < 0.05$).

Preparation and characterization of IMT-Exo

To improve the therapeutic effects of Hypo-Exo in our mouse model of MI, we enhanced their targeting specificity via surface modification. To conjugate Hypo-Exo with IMT or its scramble control, we performed a two-step reaction that is simple, rapid and flexible. First, dibenzyl cyclooctyne (DBCO) groups were introduced to the surface of Hypo-Exo

by cross-linking with DBCO-sulfo-NHS. The NHS groups were combined with amino groups on either the exosomal proteins or phosphatidylethanolamine to form covalent bonds. Second, the DBCO groups on the Exo were interacted with azide-functionalized IMT to form stable triazide linkages by copper-free click chemistry. To track the Exo, the Cy5.5-labeled azides were also conjugated to the DBCO groups. (Figure 6A).

The size distributions of unmodified and IMT modified Hypo-Exo were evaluated by nanoparticle tracking analysis (NTA), which showed that the peak of both profiles were less than 150 nm (Figure 6B). To estimate the degree to which the peptide was presented on modified Exo, a fluorescent cyclic peptide [(Cy5.5) IMT] was conjugated, and Figure 6C shows that most of the Exo were successfully conjugated with the IMT peptide compared with unmodified Hypo-Exo.

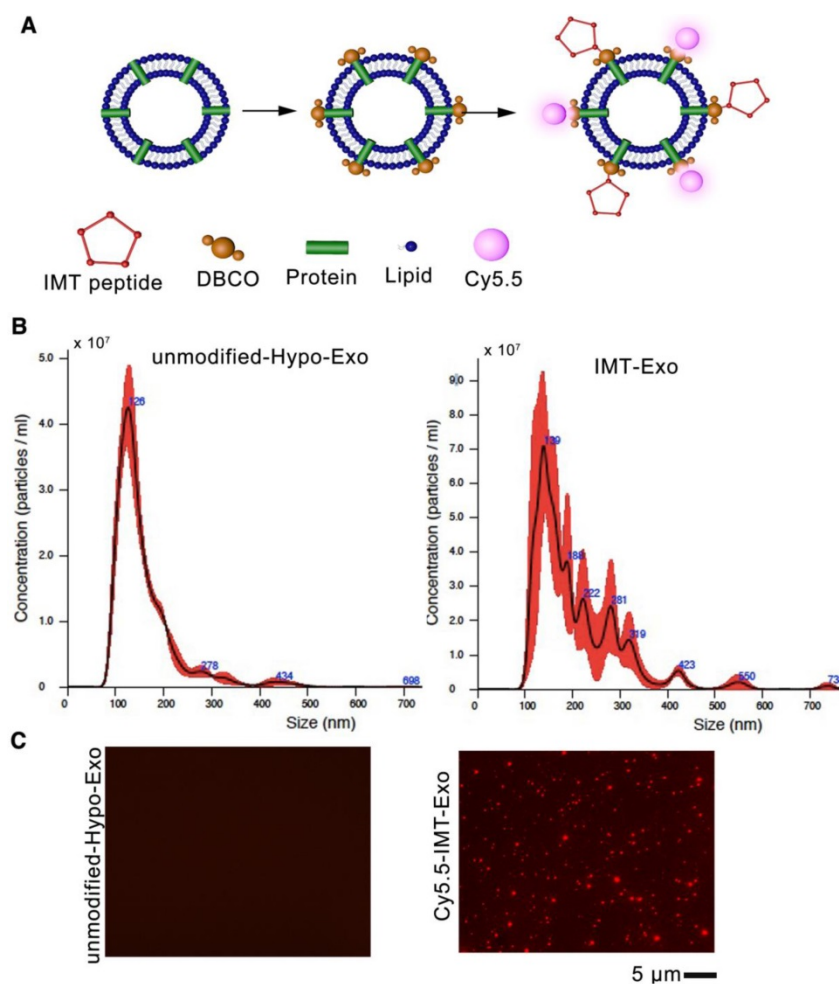


Figure 6. Characterization of targeting Hypo-Exo. (A) Schematic diagram of the conjugation of “CSTSMKAC” peptide (IMT peptide) and Cy5.5 fluorophore to exosomal amine groups by a two-step reaction. (B) Size distribution of unmodified Hypo-Exo and IMT conjugated Hypo-Exo (IMT-Exo) by NTA measurements. (C) Fluorescence images of unmodified-Hypo-Exo or Cy5.5-IMT-Exo. Red, Cy5.5. Each experiment was repeated 3 times. Scale bar, 5 μm . IMT: ischemic myocardium-targeted; IMT-Exo: IMT-conjugated Hypo-Exo; Cy5.5-IMT-Exo: Cy5.5 labeled IMT-Exo.

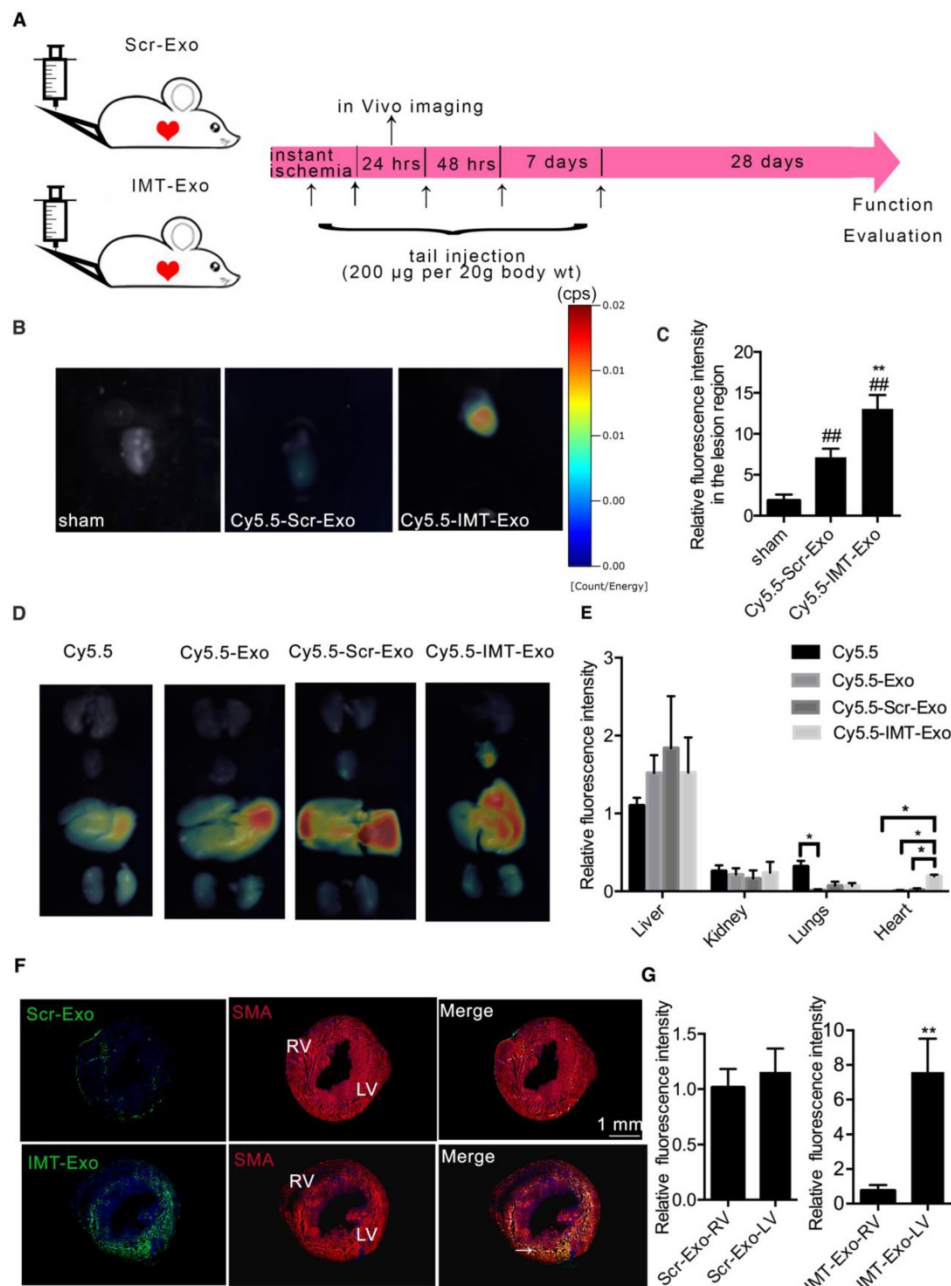


Figure 7. Ability of IMT-Exo to target the affected region of the ischemic heart. (A) Schematic representation of intravenous injection of targeting Exo in the mouse model of MI. (B) Representative *in vivo* images of mouse hearts that were subjected to MI and administered sham, Cy5.5-labeled Scramble-Hypo-Exo (Cy5.5-Scr-Exo), or Cy5.5-IMT-Exo. Hearts were dissected 24 hrs after Exo administration. (C) Quantification of the relative fluorescence intensity in the lesion region. (D) Representative *in vivo* images of organs dissected from mice that were subjected to MI and administered Cy5.5, Cy5.5-Exo, Cy5.5-Scr-Exo, or Cy5.5-IMT-Exo. Organs were dissected 24 hrs after administration. (E) Quantitation of fluorescence intensity in various organs. (F) Fluorescence images of hearts subjected to MI at 24 hrs after intravenous injection of Scr-Exo or IMT-Exo. Arrows show some of the colocalization of Exo (green) and cardiomyocytes (red). (G) Fluorescence intensity ratio of LV to RV after Scr-Exo or IMT-Exo administration. * $P < 0.05$, ** $P < 0.01$ for Cy5.5 vs. Exo in the lung; * $P < 0.05$, ** $P < 0.01$ for Cy5.5, Cy5.5-Exo, Cy5.5-Scr-Exo vs. Cy5.5-IMT-Exo in the heart; * $P < 0.05$, ** $P < 0.01$ for IMT-Exo in LV vs. RV; # $P < 0.05$, ## $P < 0.01$ for Cy5.5-Scr-Exo, Cy5.5-IMT-Exo vs. sham. LV: left ventricle; RV: right ventricle. Scr-Exo: Scrambled control modified Hypo-Exo; Cy5.5-Exo: Cy5.5 labeled Hypo-Exo; Cy5.5-Scr-Exo: Cy5.5 labeled Scr-Exo.

The ability of IMT-Exo to target the ischemic myocardium

To evaluate the ability of IMT-Exo to target ischemic myocardium *in vivo*, mice were subjected to an acute MI model, and then IMT-Exo or Scrambled control modified Hypo-Exo (Scr-Exo) was

intravenously injected immediately after surgery, 4 hrs, 24 hrs, 48 hrs post-MI, and 7 d post-MI (Figure 7A). At 24 h after MI, hearts were dissected and analyzed using an *in vivo* imaging system. As shown in Figure 7B-C, the fluorescence intensity of the injured region was significantly higher in mice administered Cy5.5-IMT-Exo than in sham controls

and in mice administered Cy5.5-Scr-Exo (13.05 ± 0.97 -fold vs. 1.84 ± 0.43 -fold and 7.15 ± 0.59 -fold; both $P < 0.01$). This result indicates that IMT conjugation significantly increases accumulation of Hypo-Exo in the lesion of the ischemic myocardium.

Next, different mouse organs (heart, lungs, liver, spleens, kidneys, e.g.) were dissected and quantitatively analyzed by an *in vivo* imaging system to observe the biodistribution of IMT-Exo. **Figure 7D-E** show that Cy5.5-Scr-Exo primarily accumulated in the liver, followed by the kidneys, lungs and the heart. Interestingly, Cy5.5-IMT-Exo injection resulted in increased accumulation in the heart compared to Cy5.5-Exo ($P < 0.05$) or Cy5.5-Scr-Exo injection ($P < 0.05$). The excessive signal accumulation in the liver of mice injected with either Cy5.5-IMT-Exo or Cy5.5-Scr-Exo is consistent with the recent report about the distribution of Cy5.5 labeled drugs after in tail injection [34].

To histologically investigate the potential for IMT-Exo to specifically target the ischemic myocardium, PKH67-labeled Scr-Exo or IMT-Exo were intravenously administered to mice subjected to MI. After 24 hrs of blood circulation, heart tissues were sectioned and analyzed by confocal microscopy. As shown in **Figure 7F-G**, PKH67-labeled IMT-Exo were primarily enriched in the ischemic myocardium of the left ventricle (LV) versus the right ventricle (RV) (11.13 ± 2.08 -fold change, $P < 0.01$); no significant differences were detected between the LV and RV of the Scr-Exo group. These results indicated that IMT-Exo, but not Scr-Exo, can target the ischemic heart and be retained in the ischemic myocardium following intravenous administration.

Cellular localization of IMT-Exo *in vitro* and *in vivo*

We further tested the ability of IMT-Exo to target hypoxia-challenged H9C2 cells, a condition to mimic ischemic injury. Cy5.5-Scr-Exo- or Cy5.5-IMT-Exo treated H9C2 cells after it was subjected to hypoxia for 2 h. As shown in **Figure 8A-B**, significantly higher fluorescence signals were observed in Cy5.5-IMT-Exo-treated hypoxia injured cells than in the Cy5.5-Scr-Exo-treated group (3.98 ± 0.32 -fold vs. 1.15 ± 0.29 -fold, $P < 0.01$). Furthermore, according to a previous report [26], the IMT peptide specifically localizes to and is retained at the ischemic myocardium after intravenous delivery due to its interaction with cardiac troponin I (cTnI), which is exposed extracellularly after MI [35]. To further verify this result *in vivo*, we assessed the accumulation of IMT-Exo in the ischemic region 24 h after intravenous injection. PKH67-labeled IMT-Exo was abundantly present in the ischemic cardiomyocytes of LV with

cTnI enrichment compared to levels in the nonischemic RV (**Figure 8C-D**, 4.96 ± 1.06 -fold vs. 0.77 ± 0.22 -fold, $P < 0.05$). These results indicated that IMT-Exo bind cTnI on myocytes and enter the lesions of the myocardium.

Intravenous injection of IMT-Exo markedly alleviates cardiac damage following MI

To confirm the therapeutic potential of IMT-Exo, we injected them via the tail vein (as shown in **Figure 7A**) immediately after MI surgery, and at 4 hrs, 24 hrs, 48 hrs and 7 days post-MI, and analyzed cardiac function on day 28. Echocardiography images indicated that the EF% and FS% were significantly higher in the IMT-Exo group than in the PBS and Scr-Exo control groups (**Figure 9A**, EF%: $47.67\% \pm 1.45\%$ vs. $28.33\% \pm 2.19\%$ and $38.33\% \pm 1.45\%$, $P < 0.01$ and $P < 0.05$, respectively; FS%: $32.33\% \pm 1.45\%$ vs. $19.33\% \pm 2.33\%$ and $24.67\% \pm 2.03\%$, $P < 0.01$ and $P < 0.05$, respectively). At the same time, Masson's trichrome staining revealed that IMT-Exo significantly reduced infarct size compared with PBS or Scr-Exo treatment (**Figure 9B**, $8.14\% \pm 1.03\%$ vs. $41.00\% \pm 7.37\%$ and $18.83\% \pm 1.82\%$, $P < 0.01$ and $P < 0.05$, respectively). Interestingly, as shown in **Figure 9C**, treatment with IMT-Exo attenuated apoptosis ($6.26\% \pm 1.17\%$ vs. $20.50\% \pm 1.63\%$ and $12.27\% \pm 1.52\%$, $P < 0.01$ and $P < 0.05$) in the BZ compared with those treated with PBS or Scr-Exo 4 weeks after MI. These results indicated that IMT-Exo achieve better cardioprotective response and promote-cardiomyocyte survival after myocardial ischemia. Finally, in order to highlight the role of MSC derived exosomal miR-125b, we modified miR125b^{KD}-Hypo-Exo with IMT peptide. **Figure S1** shows that the EF% and FS% were significantly lower in IMT-miR125b^{KD}-Hypo-Exo-treated mice than in IMT-NC-Hypo-Exo-treated mice. And, Masson's trichrome staining suggests IMT-miR125b^{KD}-Hypo-Exo significantly increased the infarct size compared with IMT-NC-Hypo-Exo.

Discussion

Although numerous strategies for MSC-based cardiac repair have been tested in patients with IHD, the benefits of such therapies in clinical trials remain modest [36]. Accumulating evidence indicates that Exo released from MSCs protect ischemic cardiomyocytes from death, promote their remodeling, and preserve cardiac function [37]. Hypoxic preconditioning of MSCs is a useful approach to increase their therapeutic potential in a mouse model of hindlimb ischemia. Our study further characterized the Exo derived from murine hypoxic MSCs, and we show that specific targeting of Exo

achieves an improved effect on cardiac recovery following MI.

Many studies employed the myocardial ischemic reperfusion (I/R) model to study cardiac therapy following ischemia. We instead used the permanent MI model because: 1. Our studies explored the representative clinical situation where MI patients are not subjected to reperfusion. 2. We focus on myocardial changes, such as remodeling, which occur over an extended period of time post-MI, whereas the I/R model is generally used to examine the short-term effects of ischemic injury [38]. 3. The effects of interventions on post-MI remodeling can be studied using nonreperfused MI that is dependent on the formation of collateral vessels but not regular capillaries as in the I/R model [39]. 4. The reperfusion procedure per se can expand the damaged area,

which introduces a confounding effect on cardiac repair.

In the current study, we analyzed miRNA content, biological effects, and cardioprotective function of Hypo-Exo *in vitro* and in a mouse model of MI. Our results show that (1) intramyocardial administration of Hypo-Exo after MI improved LV function and decreased infarction size; (2) hypoxic MSC-derived Exo were enriched with miR-125b-5p; (3) Hypo-Exo-derived miR-125b-5p documents a profound antiapoptotic effect on ischemic cardiomyocytes *in vitro* and *in vivo* via suppressing *p53* and *BAK1*; and (4) Hypo-Exo with covalently attached IMT peptide significantly improved the targeting efficiency of Exo in the ischemic heart region and reduced cardiomyocyte apoptosis post-MI.

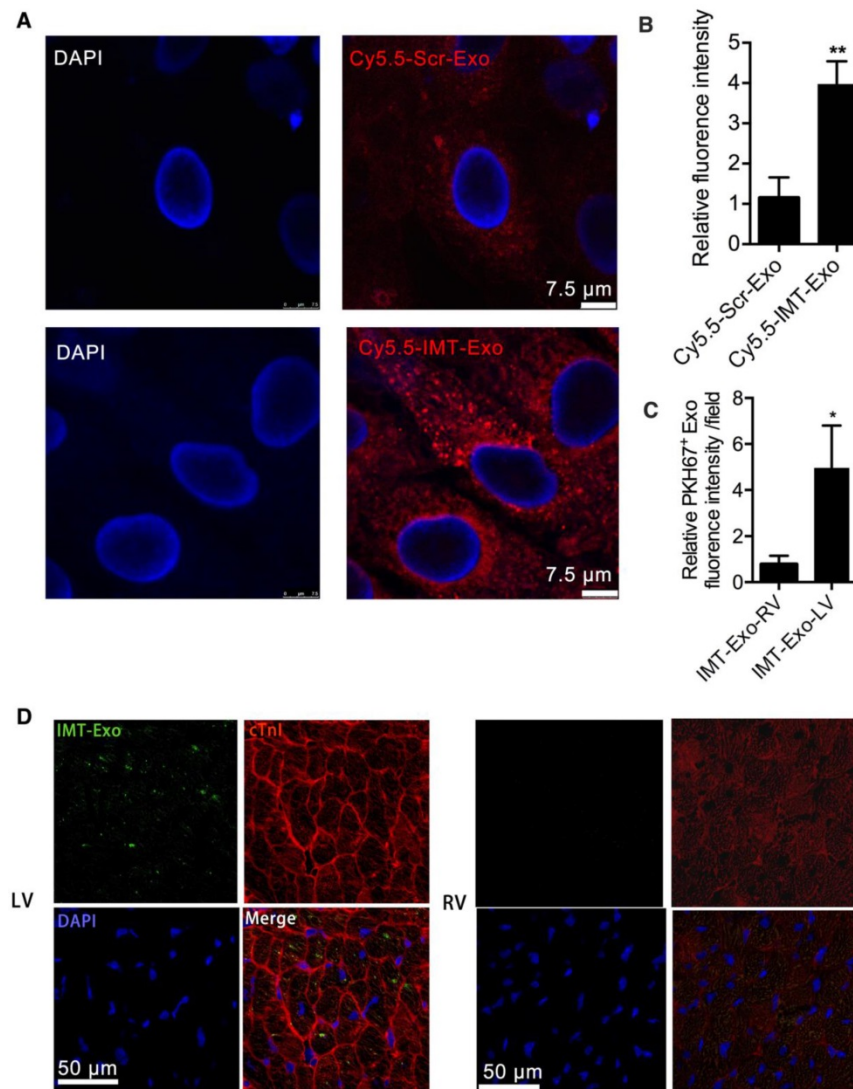


Figure 8. Evaluation of the cellular localization of IMT-Exo *in vitro* and *in vivo*. (A-B) Representative fluorescence images (A) and bar graph (B) of hypoxia-injured H9C2 cells treated with Cy5.5-Scr-Exo or Cy5.5-IMT-Exo. Scale bar, 7.5 μ m. (C-D) Bar graph (C) and colocalization images (D) of IMT-Exo (green; PKH67) with cTnI (red) in RV and LV. Scale bar, 50 μ m. Each experiment was repeated 3 times. * $P < 0.05$, ** $P < 0.01$ for Cy5.5-IMT-Exo vs. Cy5.5-Scr Exo; * $P < 0.05$, ** $P < 0.01$ for IMT-Exo in LV vs. RV.

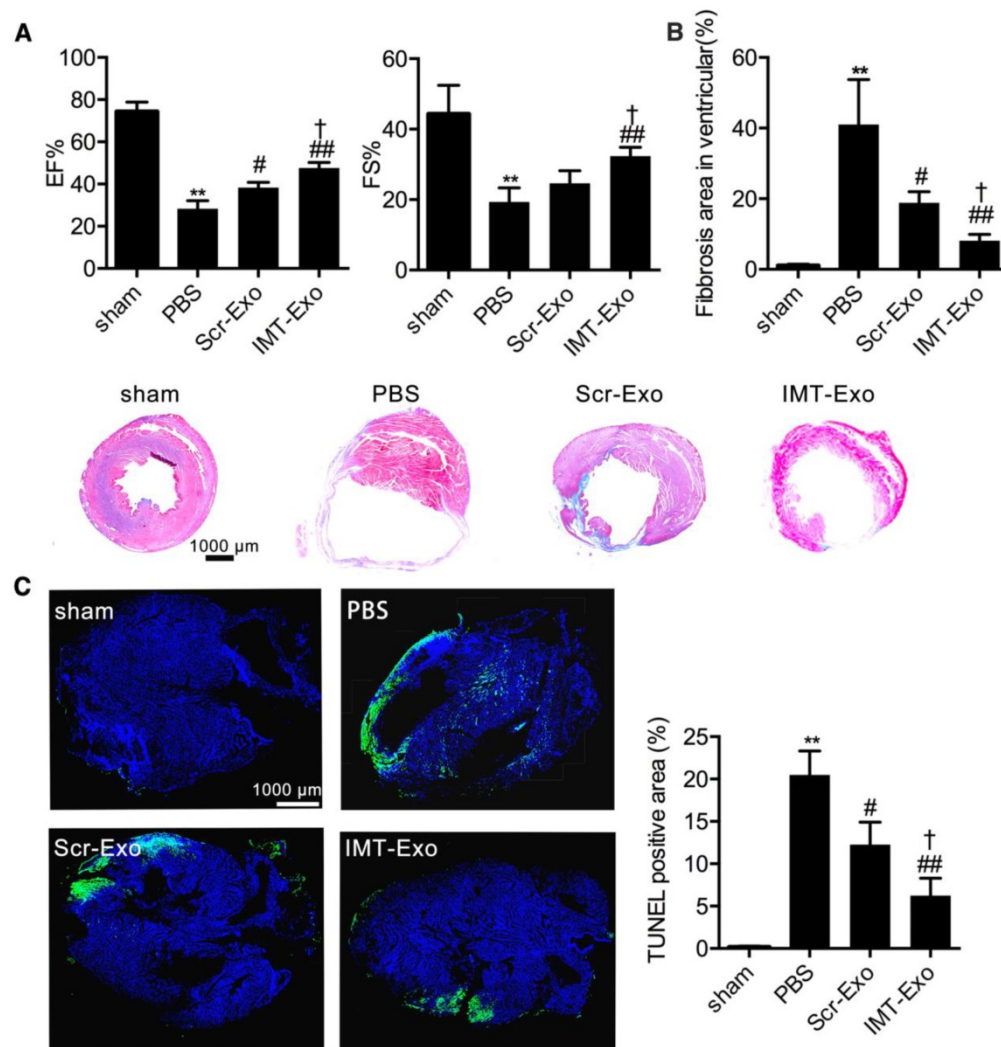


Figure 9. The role of IMT-Exo in cardiac protection post-MI. (A) Quantification of EF% and FS% measured by echocardiography of sham, PBS, Scr-Exo, and IMT-Exo groups in the mouse model of MI. **(B)** Bar graph of ventricular fibrosis and representative Masson's trichrome-stained myocardial sections of hearts from mice in the sham, PBS, Scr-Exo, and IMT-Exo groups at 28 days after MI. Scale bar, 1 mm. **(C)** Quantification and representative images of the apoptotic area in the hearts of MI model mice treated with sham, PBS, Scr-Exo, and IMT-Exo. Scale bar, 1 mm. n=6 mice per group. *P<0.05, **P<0.01 for PBS vs. sham; #P<0.05, ##P<0.01 for Scr-Exo or IMT-Exo vs. PBS; †P<0.05, ††P<0.01 for IMT-Exo vs. Scr-Exo.

Recent studies have uncovered a new cell-to-cell communication mediated by Exo, which acts as a surrogate for many of the beneficial effects of MSC [40,41]. One recent study contained proteomic analysis of Exo derived from MSCs exposed to peripheral arterial disease (PAD)-like conditions, and revealed an enrichment of proangiogenesis proteins, including the VEGF, FGF and PDGF pathways. Although the cardio-protective function of hypoxia MSC-derived Exo have been reported in some IHD studies [42], the role of miRNA in mediating Hypo-Exo function *in vivo* and *in vitro* still remains elusive. In our present study, we demonstrate for the first time that miR125b-5p in Hypo-Exo bolster ischemic heart repair and decrease the infarct size in a mouse model of MI.

Numerous studies have reported that in ischemic tissue diseases certain stem cell-originated

Exo can directly communicate with their target cells through specific miRNA. One study demonstrated that CD34-derived Exo can directly transfer stable and functional exosomal miR-126-3p to ischemic hindlimb and enhance angiogenesis by suppressing the expression of its target SPRED1[14]. Another study showed that the beneficial effects of mouse embryonic stem cell-derived Exo on cardiac progenitor cell (CPC) survival and proliferation were associated with delivery of embryonic stem cell-specific miR-294 to CPCs [43]. However, an unbiased analysis of the miRNA profile of mouse Hypo-Exo and a mechanistic study for the miRNA-mediated cardioprotective effects have not been reported. Our studies found that Hypo-Exo expressed high levels of miR-125b-5p, elevated levels of which were also observed in the BZ in ischemic heart tissue after treatment with Hypo-Exo. miR-125b-5p is a homologue of lin-4,

which was the first miRNA discovered and is an important regulator of *C. elegans* development [44]. miR-125b-5p impedes apoptosis by repressing *p53* and *BAK1* expression. Furthermore, increased expression of miR-125b-5p in macrophages attenuates hypoxia/reperfusion -induced cell injury. Increased expression of miR-125b-5p in the myocardium significantly reduces myocardial infarct size and prevents I/R-induced cardiac dysfunction [32]. Consistent with this, we observed that treatment with miR-125b^{KD}-Hypo-Exo impaired the survival of ischemic cardiomyocytes *in vitro* and *in vivo* by increasing the expression of miR-125b-5p target genes *p53* and *BAK1*. Thus, exosomal miR-125b-5p exerts a cardioprotective function in myocardial infarction by downregulating the expression of apoptotic genes *p53* and *BAK1*. These results are in concordance with studies reporting that miR-125b modulates cardiomyocyte proliferation and survival [32,33]. One recent study indicates that miR-125b-5p is critical for fibroblast-to-myofibroblast differentiation. In that study, miR-125b-5p inhibited *p53* to induce fibroblast proliferation, which exacerbated MI-induced scarring in an AngII infusion-induced cardiac fibrosis mouse model [45]. Fibrosis is the pathological end point of both hypertension overload and I/R; the two distinct pathological progresses may contribute to the different roles of miR-125b-5p. For instance, hypertension overload-induced reactive cardiac fibrogenesis was initiated by increased stress in the myocardial wall, whereas our study induced fibrosis via cardiomyocyte death due to MI. Thus, it is not surprising that the regulation of miR-125b is dependent on its environment. Additionally, we cannot exclude contributions from other miRNAs in Hypo-Exo, alone or in combination, to the anti-apoptosis and therapeutic effects. The complete molecular content of Hypo-Exo and the underlying mechanism of its cardioprotective function will be explored in our future studies.

Hypo-Exo is considered a promising therapeutic approach for tissue ischemia; however, specific targeting of Exo to the ischemic heart remains a challenge following systemic delivery. Our previous study applied a universal strategy to modify the Exo surface with the c(RGDyK) peptide via bio-orthogonal chemistry, and the resulting Exo specifically targeted brain ischemic lesions [24]. Inspired by this “Exo engineering” method, we modified Hypo-Exo in this study with the IMT peptide so that it will preferentially target ischemic-injured cardiomyocytes and minimize possible off-target side effects. Although the size of Exo is increased after modification, IMT-Exo maintain an intact vesicle shape and show pronounced targeting efficiency in

our mouse MI model. Our results suggest that the targeting specificity of IMT-Exo was achieved by its interaction with cTnI, which is specifically expressed in ischemic myocytes and is released into the extracellular matrix [35]. Our results are consistent with a previous study that applied IMT-VEGF to enhance angiogenesis and improve cardiac function in a rat I/R injury model [26].

In conclusion, our studies highlight a novel mechanism by which cell-free Hypo-Exo facilitate ischemic heart repair via the antiapoptotic miR-125b-5p. Furthermore, we report a novel, rapid and safe method to modify Hypo-Exo to improve their selective targeting to ischemic heart tissue, which increased their therapeutic efficiency in a mouse MI model.

Abbreviations

BZ: border zone; CPCs: cardiac progenitor cells; cTnI: cardiac troponin I; DZ: distant zone; EF%: ejection fraction; ESCV: end systolic chamber volume; Exo: exosomes; FS%: fractional shortening; Hypo-Exo: hypoxia-conditioned bone marrow mesenchymal stem cell- derived exosomes; IHD: ischemic heart disease; IMT: ischemic myocardium-targeted; I/R: myocardial ischemic reperfusion; KD: knockdown; LA: left ventricle; LSM: laser scattering microscopy; LVID: left ventricular internal diameter; MI: myocardial infarction; miRNA: microRNA; MPS: mononuclear phagocyte system; MSC: mesenchymal stem cell; Nor-Exo: normoxia-conditioned bone marrow mesenchymal stem cell-derived exosomes; RV: right ventricle; Scr-Exo: scrambled control modified hypoxia-conditioned bone marrow mesenchymal stem cell- derived exosomes.

Acknowledgements

This study was supported by grants from the National Natural Science Foundation of China (No. 81570239, 81770301, 81670267) and the National Basic Research Program of China (973 Program, No. 2014CB542402). This Work was supported by Grants from the Project of Innovation-driven Plan in Central South University (No. 2016CX5023) and excellent young scientist foundation of NSFC (81822004).

Author Contributions

YPB conceived and funded this study. GGZ conceived ideas for the experimental designs, analyzed the data and prepared the manuscript. LPZ conducted the majority of the experiments. TT and HXZ performed IMT-Exos construction and labeling dye. JYW, JNH and MP performed Exo isolation. XTQ and LX performed some *in vitro* and animal experiments. TC, CCL, KKW and HS analyzed some

data. We thank Dr. LHF at Houston Methodist Research Institute for revising this manuscript.

Supplementary Material

Supplementary method and figures.

<http://www.thno.org/v08p6163s1.pdf>

Competing Interests

The authors have declared that no competing interest exists.

References

- Bayés de Luna A, Guindo J. Sudden death in ischemic heart disease. *Rev Port Cardiol.* 1990; 9(5): 473-9.
- Li C, Zhen G, Chai Y, Xie L, Crane JL, Farber E, et al. RhoA determines lineage fate of mesenchymal stem cells by modulating CTGF-VEGF complex in extracellular matrix. *Nat Commun.* 2016; 7: 11455.
- Orlic D, Kajstura J, Chimenti S, Jakoniuk I, Anderson SM, Li B, et al. Bone marrow cells regenerate infarcted myocardium. *Nature.* 2001; 410(6829): 701.
- Kurtz A. Mesenchymal stem cell delivery routes and fate. *Int J Stem Cells.* 2008; 1(1): 1.
- Lin KC, Yip HK, Shao PL, Wu SC, Chen KH, Chen YT, et al. Combination of adipose-derived mesenchymal stem cells (ADMSC) and ADMSC-derived exosomes for protecting kidney from acute ischemia-reperfusion injury. *Int J Cardiol.* 2016; 216: 173-85.
- Kim DK, Nishida H, An SY, Shetty AK, Bartosh TJ, Prockop DJ. Chromatographically isolated CD63+ CD81+ extracellular vesicles from mesenchymal stromal cells rescue cognitive impairments after TBI. *Proc Natl Acad Sci U S A.* 2016; 113(1): 170-5.
- Kalluri R. The biology and function of exosomes in cancer. *J Clin Invest.* 2016; 126(4): 1208-15.
- Tkach M, Théry C. Communication by extracellular vesicles: where we are and where we need to go. *Cell.* 2016; 164(6): 1226-32.
- Hu Y, Rao SS, Wang ZX, Cao J, Tan YJ, Luo J, et al. Exosomes from human umbilical cord blood accelerate cutaneous wound healing through miR-21-3p-mediated promotion of angiogenesis and fibroblast function. *Theranostics.* 2018; 8(1): 169.
- Li Y, Cheng Q, Hu G, Deng T, Wang Q, Zhou J, et al. Extracellular vesicles in mesenchymal stromal cells: A novel therapeutic strategy for stroke. *Exp Ther Med.* 2018; 15(5): 4067-79.
- Chen CY, Rao SS, Ren L, Hu XK, Tan YJ, Hu Y, et al. Exosomal DMBT1 from human urine-derived stem cells facilitates diabetic wound repair by promoting angiogenesis. *Theranostics.* 2018; 8(6): 1607.
- Shuijter JP, Davidson SM, Boulanger CM, Buzás EI, de Kleijn DP, Engel FB, et al. Extracellular vesicles in diagnostics and therapy of the ischaemic heart: Position Paper from the Working Group on Cellular Biology of the Heart of the European Society of Cardiology. *Cardiovasc Res.* 2017; 114(1): 19-34.
- Barile L, Cervio E, Lionetti V, Milano G, Ciullo A, Biemmi V, et al. Cardioprotection by cardiac progenitor cell-secreted exosomes: role of pregnancy-associated plasma protein-A. *Cardiovasc Res.* 2018; 114(7): 992-1005.
- Mathiyalagan P, Liang Y, Kim D, Misener S, Thorne T, Kamide CE, et al. Angiogenic mechanisms of human CD34+ stem cell exosomes in the repair of ischemic hindlimb. *Circ Res.* 2017; 120(9): 1466-76.
- Rosova I, Dao M, Capoccia B, Link D, Nolte JA. Hypoxic preconditioning results in increased motility and improved therapeutic potential of human mesenchymal stem cells. *Stem cells.* 2008; 26(8): 2173-82.
- Anderson JD, Johansson HJ, Graham CS, Vesterlund M, Pham MT, Bramlett CS, et al. Comprehensive proteomic analysis of mesenchymal stem cell exosomes reveals modulation of angiogenesis via nuclear factor-kappaB signaling. *Stem Cells.* 2016; 34(3): 601-13.
- Ingato D, Lee JU, Sim SJ, Kwon YJ. Good things come in small packages: Overcoming challenges to harness extracellular vesicles for therapeutic delivery. *J Control Release.* 2016; 241: 174-85.
- Armstrong JP, Holme MN, Stevens MM. Re-engineering extracellular vesicles as smart nanoscale therapeutics. *ACS nano.* 2017; 11(1): 69-83.
- Lai CP, Mardini O, Ericsson M, Prabhakar S, Maguire CA, Chen JW, et al. Dynamic biodistribution of extracellular vesicles in vivo using a multimodal imaging reporter. *ACS nano.* 2014; 8(1): 483-94.
- Wiklander OP, Nordin JZ, O'Loughlin A, Gustafsson Y, Corso G, Mäger I, et al. Extracellular vesicle in vivo biodistribution is determined by cell source, route of administration and targeting. *J Extracell Vesicles.* 2015; 4(1): 26316.
- Vandergriff A, Huang K, Shen D, Hu S, Hensley MT, Caranasos TG, et al. Targeting regenerative exosomes to myocardial infarction using cardiac homing peptide. *Theranostics.* 2018; 8(7): 1869.
- Bei Y, Das S, Rodosthenous RS, Holvoet P, Vanhaverbeke M, Monteiro MC, et al. Extracellular vesicles in cardiovascular theranostics. *Theranostics.* 2017; 7(17): 4168.
- Antes TJ, Middleton RC, Luther KM, Ijichi T, Peck KA, Liu WJ, et al. Targeting extracellular vesicles to injured tissue using membrane cloaking and surface display. *J Nanobiotechnology.* 2018; 16(1): 61.
- Tian T, Zhang HX, He CP, Fan S, Zhu YL, Qi C, et al. Surface functionalized exosomes as targeted drug delivery vehicles for cerebral ischemia therapy. *Biomaterials.* 2018; 150: 137-49.
- Cohen M, Boiangiu C, Abidi M. Therapy for ST-segment elevation myocardial infarction patients who present late or are ineligible for reperfusion therapy. *J Am Coll Cardiol.* 2010; 55(18): 1895-906.
- Yang Y, Shi C, Hou X, Zhao Y, Chen B, Tan B, et al. Modified VEGF targets the ischemic myocardium and promotes functional recovery after myocardial infarction. *J Control Release.* 2015; 213: 27-35.
- Théry C, Amigorena S, Raposo G, Clayton A. Isolation and characterization of exosomes from cell culture supernatants and biological fluids. *Curr Protoc Cell Biol.* 2006; 30(1): 3-22.
- Rutherford SC, Fachel AA, Li S, Sawh S, Muley A, Ishii J, et al. Extracellular vesicles in DLBCL provide abundant clues to aberrant transcriptional programming and genomic alterations. *Blood.* 2018; 132(7): e13-23.
- Kolk MV, Meyberg D, Deuse T, Tang-Quan KR, Robbins RC, Reichenspurner H, et al. LAD-ligation: a murine model of myocardial infarction. *J Vis Exp.* 2009; (32): e1438.
- Willimott S, Wagner SD. miR-125b and miR-155 contribute to BCL2 repression and proliferation in response to CD40 ligand (CD154) in human leukemic B-cells. *J Biol Chem.* 2012; 287(4): 2608-17.
- Le MT, Teh C, Shyh-Chang N, Xie H, Zhou B, Korzh V, et al. MicroRNA-125b is a novel negative regulator of p53. *Genes Dev.* 2009; 23(7): 862-76.
- Wang X, Ha T, Zou J, Ren D, Liu L, Zhang X, et al. MicroRNA-125b protects against myocardial ischaemia/reperfusion injury via targeting p53-mediated apoptotic signalling and TRAF6. *Cardiovasc Res.* 2014; 102(3): 385-95.
- Li Q, Wu Y, Zhang Y, Sun H, Lu Z, Du K, et al. miR-125b regulates cell progression in chronic myeloid leukemia via targeting BAK1. *Am J Transl Res.* 2016; 8(2): 447.
- Hue JJ, Lee HJ, Jon S, Nam SY, Yun YW, Kim JS, et al. Distribution and accumulation of Cy5. 5-labeled thermally cross-linked superparamagnetic iron oxide nanoparticles in the tissues of ICR mice. *J Vet Sci.* 2013; 14(4): 473-9.
- Streng AS, Jacobs LH, Schwenk RW, Cardinaels EP, Meex SJ, Glatz JF, et al. Cardiac troponin in ischemic cardiomyocytes: intracellular decrease before onset of cell death. *Exp Mol Pathol.* 2014; 96(3): 339-45.
- Afzal MR, Samanta A, Shah ZI, Jeevanantham V, Abdel-Latif A, Zuba-Surma EK, et al. Adult bone marrow cell therapy for ischemic heart disease: evidence and insights from randomized controlled trials. *Circ Res.* 2015; 117(6): 558-75.
- Barile L, Lionetti V, Cervio E, Matteucci M, Gherghiceanu M, Popescu LM, et al. Extracellular vesicles from human cardiac progenitor cells inhibit cardiomyocyte apoptosis and improve cardiac function after myocardial infarction. *Cardiovasc Res.* 2014; 103(4): 530-41.
- Gao E, Lei YH, Shang X, Huang ZM, Zuo L, Boucher M, et al. A novel and efficient model of coronary artery ligation and myocardial infarction in the mouse. *Circ Res.* 2010; 107(12): 1445-53.
- Lindsey ML, Bolli R, Canty Jr JM, Du XJ, Frangogiannis NG, Frantz S, et al. Guidelines for experimental models of myocardial ischemia and infarction. *Am J Physiol Heart Circ Physiol* 2018; 314(4): H812-38.
- Li J, Fu LZ, Liu L, Xie F, Dai RC. Glucagon-Like Peptide-1 (GLP-1) Receptor Agonist Liraglutide Alters Bone Marrow Exosome-Mediated miRNA Signal Pathways in Ovariectomized Rats with Type 2 Diabetes. *Med Sci Monit.* 2017; 23: 5410.
- Bian S, Zhang L, Duan L, Wang X, Min Y, Yu H. Extracellular vesicles derived from human bone marrow mesenchymal stem cells promote angiogenesis in a rat myocardial infarction model. *J Mol Med.* 2014; 92(4): 387-97.
- Gonzalez-King H, Garcia NA, Ontoria-Oviedo I, Ciria M, Montero JA, Sepúlveda P. Hypoxia Inducible Factor-1 α Potentiates Jagged 1-Mediated Angiogenesis by Mesenchymal Stem Cell-Derived Exosomes. *Stem Cells.* 2017; 35(7): 1747-59.
- Khan M, Nickoloff E, Abramova T, Johnson J, Verma SK, Krishnamurthy P, et al. Embryonic stem cell-derived exosomes promote endogenous repair mechanisms and enhance cardiac function following myocardial infarction. *Circ Res.* 2015; 117(1): 52-64.
- Olsen PH, Ambros V. The lin-4 regulatory RNA controls developmental timing in *Caenorhabditis elegans* by blocking LIN-14 protein synthesis after the initiation of translation. *Dev Biol.* 1999; 216(2): 671-80.
- Nagpal V, Rai R, Place AT, Murphy SB, Verma SK, Ghosh AK, et al. MiR-125b is critical for fibroblast-to-myofibroblast transition and cardiac fibrosis. *Circulation.* 2015; 133(3): 291-301.